DMD # 71142

Title Page:

Discovery of a Novel Microsomal Epoxide Hydrolase Catalyzed Hydration of a Spiro Oxetane

Xue-Qing Li, Martin A. Hayes, Gunnar Grönberg, Kristina Berggren, Neal Castagnoli Jr., and Lars Weidolf

Cardiovascular and Metabolic Diseases, Innovative Medicines and Early Development Biotech Unit, AstraZeneca, Pepparedsleden 1, Mölndal, 431 83, Sweden, (X-Q.L., M.A.H., L.W.)

Respiratory, Inflammation and Autoimmune Disease, Innovative Medicines and Early Development Biotech Unit, AstraZeneca, Pepparedsleden 1, Mölndal, 431 83, Sweden, (G.G., K.B.)

Department of Chemistry, Virginia Tech, Blacksburg, VA 24061-0001, USA (N.C.J.)

1

DMD # 71142

Running Title: Microsomal epoxide hydrolase catalyzed hydration of an oxetane

Corresponding author and contact information:

Xue-Qing Li, PhD.

Cardiovascular and Metabolic Diseases, DMPK, Innovative Medicines and Early Development

Biotech Unit, AstraZeneca, Pepparedsleden 1, Mölndal, 431 83, Sweden

Telephone: +46 31 706 5506

Fax: +46 31 776 3867

Email: xueqing.li@astrazeneca.com

Number of text pages: 31

Number of Tables: 0 (1 additional table in supplemental file)

Number of Figures: 9 (4 additional figures in supplemental file)

Number of References: 44

Number of words in Abstract: 232

Number of words in Introduction: 511

Number of words in Discussion: 1500

List of abbreviations

AO, aldehyde oxidase; AZD1979, (3-(4-(2-oxa-6-azaspiro[3.3]heptan-6-ylmethyl)phenoxy)azetidin-1-yl)(5-(4-ethoxyphenyl)-1,3,4-oxadiazol-2-yl)methanone; AZ13478123, 3-(4-{[3,3-bis(hydroxymethyl)azetidin-1-yl]methyl}phenoxy)azetidin-1-yl][5-(4-methoxyphenyl)-1,3,4-oxadiazol-2-yl]methanone; ESI, electrospray ionization; FMO, flavin-containing monooxygenase; GST, glutathione *S*-transferase; HLM, human liver microsomes; MAO, monoamine oxidase; MCHr1, melanin-concentrating hormone receptor 1; mEH, microsomal epoxide hydrolase; P450, cytochrome P450; SULT, sulfotransferase; sEH, soluble epoxide hydrolase; *t*-AUCB, trans-4-[4-(1-adamantylcarbamoylamino)cyclohexyloxy]benzoic acid; UGT, UDP-glucuronosyltransferase; UPLC/HRMS, ultra-high performance liquid chromatography/ high resolution mass spectrometry.

2

Abstract

Oxetane moieties are increasingly being used by the pharmaceutical industry as building blocks in drug candidates due to their pronounced ability to improve physicochemical parameters and metabolic stability of drug candidates. The enzymes that catalyze the biotransformation of the oxetane moiety are, however, not well studied. The in vitro metabolism of a spiro oxetane-containing compound AZD1979 was studied and one of its metabolites, M1, attracted our interest because its formation was NAD(P)H-independent. The focus of the current work was to elucidate the structure of M1 and to understand the mechanism(s) of its formation. We established that M1 was formed *via* hydration and ring opening of the oxetanyl moiety of AZD1979. Incubations of AZD1979 using various human liver subcellular fractions revealed that the hydration reaction leading to M1 occurred mainly in the microsomal fraction. The underlying mechanism as a hydration rather than an oxidation reaction was supported by the incorporation of ^{18}O from $H_2^{18}O$ into M1. Enzyme kinetics were performed probing the formation of M1 in human liver microsomes. The formation of M1 was substantially inhibited by progabide, a microsomal epoxide hydrolase inhibitor, but not by *t*-AUCB, a soluble epoxide hydrolase inhibitor. Based on these results we propose that microsomal epoxide hydrolase catalyzes the formation of M1. The substrate specificity of microsomal epoxide hydrolase should therefore be expanded to include not only epoxides, but also the oxetanyl ring system present in AZD1979.

DMD # 71142

Introduction

Drug metabolism studies on small molecule pharmaceuticals are conducted during drug

discovery and development to address issues related to biodisposition and toxicity. Such

biotransformation reactions are mediated by a vast array of enzymes, mainly present in the liver.

The cytochrome P450s (P450s) are monooxygenases that mediate the metabolism of the majority

of lipophilic drugs in clinical use (Rendic and Guengerich, 2015). The importance of non-P450

drug-metabolizing enzymes has also been highlighted, e.g. flavin-containing monooxygenases

(FMOs) (Usmani et al., 2012), monoamine oxidases (MAOs) (Inoue et al., 1999), aldehyde

oxidase (AO) (Hutzler et al., 2013), epoxide hydrolases (EHs) (Fretland and Omiecinski, 2000)

and conjugating enzymes, e.g., glutathione *S*-transferases (GSTs) (Wu and Dong, 2012),

sulfotransferases (SULTs) (Schwaninger et al., 2011) and UDP-glucuronosyltransferases (UGTs)

(Radominska-Pandya et al., 1999). Some of these non-P450 enzymes are not commercially

available and, thus, assessment of their contribution to the biotransformation of new chemical

entities can be a challenge in drug discovery.

AZD1979, (3-(4-(2-oxa-6-azaspiro[3.3]heptan-6-ylmethyl)phenoxy)azetidin-1-yl)(5-(4-

ethoxyphenyl)-1,3,4-oxadiazol-2-yl)methanone, is a melanin-concentrating hormone receptor 1

(MCHr1) antagonist designed for the treatment of obesity. A spiro oxetanylazetidinyl moiety

was introduced as a building block in AZD1979 resulting in favorable physicochemical and

pharmacokinetic properties in comparison to other 4-, 5- or 6-membered ring systems

investigated (Johansson et al., 2016). Similarly, the use of oxetanes was shown to improve the

human microsomal stability of drug-like compounds (Burkhard et al., 2013; Scott et al., 2013).

However, only a limited number of studies have been published on the metabolism of oxetanes.

Rioux et al. (Rioux et al., 2016) reported a CYP2D and 3A mediated oxidative ring scission

pathway of a 3-substituted oxetanyl containing compound EPZ015666 and Stepan et al. (Stepan et al., 2011) reported that members of an oxetanyl series of derivatives undergo oxidation of the cyclic ether moiety. In both studies, the P450-catalyzed oxidation took place on the carbon α to the oxygen atom, leading to unstable hemiacetal intermediates. This was followed by conversion to the corresponding ring opened aldehydes and further reduction to the corresponding diols or oxidation to the carboxylic acids.

The metabolism of AZD1979 represents an interesting case study of the metabolism of a 3-substituted spiro oxetane-containing drug candidate. Considering the specific properties of the strained spiro oxetanylazetidinyl moiety in AZD1979 and the increasing interest in incorporating spirocycles as scaffolds in drug design (Wuitschik et al., 2008; Stepan et al., 2011; Carreira and Fessard, 2014; Zheng et al., 2014), it was of particular interest to characterize the metabolic pathways of this compound and the enzymology contributing to its clearance. In this study, we describe the non-P450-mediated formation of a metabolite M1 of AZD1979 and its structural characterization. It was shown that M1 was formed by hydrative ring cleavage of the oxetanyl moiety of the spiro system of AZD1979. We also report the identification of liver microsomal EH (mEH) as the enzyme that catalyzes the formation of M1 and propose an underlying mechanism. The discovery that this four-membered oxetane is a substrate of mEH broadens the reported substrate specificity of this enzyme and adds further understanding to the importance of this novel metabolic pathway in drug research.

Materials and Methods

Chemicals and reagents. AZD1979, progabide, and *trans*-4-[4-(1-adamantylcarbamoylamino)cyclohexoxy]benzoic acid (*t*-AUCB) were obtained from AstraZeneca Compound Management (AstraZeneca R&D Gothenburg, Sweden). [^{14}C]-labelled AZD1979 was obtained from Isotope Chemistry, AstraZeneca R&D Gothenburg, Sweden. $H_2^{18}O$ (97 atom % ^{18}O), NADPH and NADH were purchased from Sigma Aldrich (St. Louis, MO, USA). All other chemicals and solvents were of the highest quality commercially available. Pooled human liver microsomes (HLM) were purchased from BD Gentest (Woburn, MA, USA). Pooled human liver cytosol and S9 fraction were purchased from XenoTech, LLC (Lenexa, KS, USA).

Synthesis of AZ13478123. The oxetanyl ring opened diol analogue of AZD1979 was synthesized as follows. To a round-bottom flask AZD1979 (200 mg), 1,4-dioxane (8 mL) and H_2SO_4 (410 µL, 0.3 M) were added at decreased temperature followed by the addition of a second portion of dioxane (4 mL). The mixture was stirred at room temperature for 1 hour and then heated at 75°C for 1 hour. The reaction mixture was cooled to room temperature and diluted with ethyl acetate (5 mL), basified by $NaHCO_3$ (2 mL aq., 5%) and solid $NaHCO_3$. The separated organic phase was dried (Na_2SO_4), filtered and the solvent was evaporated at reduced pressure. The crude product was purified by preparative HPLC on an XBridge C_{18} column (10 µm, 250 × 19 mm, Waters). A mobile phase consisting of A) acetonitrile and B) H_2O/ACN/NH_3 (95/5/0.2, v/v) was used. A gradient was used from 20% A as initial conditions increasing to 60% over 40 min. A flow rate of 19 mL/min and UV detection at 292 nm were used. The desired fractions were combined and the solvents were evaporated under reduced pressure. The residue was extracted in dichloromethane, dried through a phase separator and the solvent was

evaporated at reduced pressure to yield AZ13478123 as a white solid (30 mg, Yield=14%). High

resolution mass spectrometry (HRMS): the m/z of the MH$^+$ ion ($C_{25}H_{29}N_4O_6$) was calculated as

481.2082 and found at 481.2097. The NMR assignments of AZ13478123 were compared to the

fully assigned ^{1}H and ^{13}C spectra of AZD1979. The details of the NMR characterization of

AZ13478123 are provided in the Supplemental Data.

Incubations in human liver subcellular fractions. In general, compound AZD1979 was

incubated with HLM, cytosol or S9 fraction (0.5 or 1 mg protein/mL) in 0.1 M potassium

phosphate buffer (pH 7.4) containing MgCl$_2$ (3 mM). The incubations were performed in 96-well

plates with a total volume of 200 µL/well in a shaking incubator at 37 °C. All samples were

preincubated for 5 minutes, and then reactions were initiated by addition of AZD1979. Control

incubations to examine the chemical stability of AZD1979 were performed in buffer without the

addition of enzymes. Following a defined incubation time, aliquots (50 µL) of the incubation

mixture were quenched by mixing with ice-cold acetonitrile (100 µL). After centrifugation at

4,500 g for 20 min, a 50 µL aliquot of the supernatant was diluted with 100 µL water and the

resulting mixture was analyzed by ultra-high performance liquid chromatography/ high

resolution mass spectrometry (UPLC/HRMS). All incubations were carried out in duplicate

throughout the study.

In the NAD(P)H-dependence study, a mixture of NADPH and NADH (both 1.0 mM and referred

to as NAD(P)H) was added into the AZD1979 (10 µM) incubation mixture and incubated for 0

and 60 min. A protein concentration of 1 mg/mL of HLM, cytosol or S9 was used. In parallel, a

set of control samples were incubated using the similar condition but without the addition of

NAD(P)H.

In the pH-dependence study, AZD1979 (50 µM) was incubated with HLM or S9 fraction (1 mg/mL protein) in 0.1 M potassium phosphate buffer at pH 6.5, 7.4, 8.5 and 9.0 for 60 min.

Time course of incorporation of ^{18}O from $H_2^{18}O$ into metabolite M1. Incorporation of ^{18}O-labeled water (77.6% ^{18}O, taking in account the 80% $H_2^{18}O$ (97 atom % ^{18}O) and the amount of unlabeled buffer and liver fractions in the incubations) into metabolite M1 was assessed by incubation of AZD1979 (10 µM) in human liver S9 fraction and HLM (1 mg/mL protein) under the conditions described earlier. Reactions were terminated at 0, 30, 60 and 120 min by adding 50 µL aliquots of incubation mixture to 100 µL ice-cold acetonitrile. After mixing, all samples were centrifuged and the resulting supernatants were diluted with 2 volumes of unlabeled water before UPLC/HRMS analysis. The amounts of ^{18}O incorporated in metabolite M1 were calculated using the metabolite isotopic profiles and correcting for naturally occurring isotopic species, as determined from the corresponding spectra of the metabolite obtained in $H_2^{16}O$ incubations. Synthesized unlabeled M1 (AZ13478123) was incubated in $H_2^{18}O$ (77.6% ^{18}O) for 60 and 120 min as a control. UPLC/HRMS analysis provided an estimate of the extent to which M1 undergoes spontaneous exchange with $H_2^{18}O$.

Enzyme kinetic studies. Incubations in HLM were used to examine the kinetics of the enzyme-catalyzed hydration of AZD1979. Linear conditions of the rate of M1 formation from AZD1979, identified by comparison with synthesized AZ13478123, with respect to time and protein concentration were determined in HLM. Enzyme kinetics of M1 formation were performed at a protein concentration of 1 mg/mL for 30 min and at substrate concentrations ranging from 20 – 600 µM. K_m and V_{max} values were calculated by nonlinear regression analysis of all individual data points using Enzyme Kinetics implemented in SigmaPlot version 13.0 (Systat Software, San Jose, CA).

Inhibition of M1 formation in HLM, liver S9 fraction and cytosol by inhibitors of epoxide hydrolase. The effect of the mEH inhibitor progabide on the rate of M1 formation was examined in HLM (0.5 mg/mL protein), S9 fraction (1 mg/mL protein) or cytosol (1 mg/mL protein) following 0, 30, 60 and 120 min incubation of AZD1979 (10 µM) in the presence of progabide at 0, 20, 50 and 100 µM. The extent of inhibition of M1 at 60 minutes by the soluble EH (sEH) inhibitor t-AUCB was also examined in all three liver subcellular fractions at a t-AUCB concentration (10 µM) that should result in complete inhibition of sEH activity (Hwang et al., 2007). Furthermore, an experiment to determine the IC_{50} value of progabide on M1 formation was performed in HLM (1 mg/mL protein) at an AZD1979 concentration of 200 µM and at concentrations of progabide ranging from 0 to 100 µM. The incubation time was 30 minutes. The IC_{50} value was calculated by nonlinear fit using Grafit (version 5.0.13).

UPLC/HRMS analysis of M1. LC separations were performed on an Acquity UPLC BEH C_{18} column (2.1×100 mm, 1.7 µm; Waters, Milford, MA) operated by an Acquity UPLC system (Waters). Mobile phase A was 0.1% formic acid in water and mobile phase B was acetonitrile. The initial mobile phase was 90:10 A-B, transitioning to 60:40 A-B over 6 mins using a linear gradient. The flow rate was 0.5 mL/min. The total run time was 7 minutes and the column oven was set to 45°C. The UPLC eluent was introduced into a Xevo Q-TOF mass spectrometer (Waters) with an electrospray ionization (ESI) interface and operated in the positive ESI mode with MS resolving powers of 20,000. Specific mass spectrometric source conditions were as follows: capillary voltage of 0.5 kV, sample cone voltage of 30 V, desolvation temperature of 450 °C. Mass spectra were acquired over the range m/z 80–1200. MS/MS spectra of the MH^+ ions of AZD1979 and M1, respectively, were obtained for structure identification using a cone voltage of 20 V, a collision energy ramped from 15 to 35 eV, and a transfer collision energy of

15 eV. In the analysis, the extracted ion MS chromatograms at *m/z* 481.2087 (M1) were

generated and processed by TargetLynx (Waters) with a mass tolerance of 20 mDa. The peak

area corresponding to M1 was used for semi-quantification. In the study of ^{18}O incorporation

into M1, extracted ion chromatograms at *m/z* 483.2130 ([^{18}O]M1) were also processed and peak

areas corresponding to [^{18}O]M1 were integrated. Quantitative analyses on kinetic studies of M1

formation were performed using a reference standard curve constructed with concentrations of

synthesized AZ13478123 from 0.01 to 3 µM. The entire unit was operated using MassLynx

(version 4.1). The UPLC/HRMS properties of the synthesized reference were identical to those

of metabolite M1 except for the expected mass shifts for the ^{18}O-incorporated metabolite.

Results

Structural characterization of hydrated metabolite M1. Following incubations of AZD1979

in HLM with and without the addition of a mixture of NADPH and NADH (NAD(P)H), several

metabolites were detected in the presence of NAD(P)H. The most significant metabolite of

AZD1979 was a phenol formed *via O*-demethylation (structure of AZD1979 shown in Figure 1).

An *N*-oxide and a hydrated metabolite (M1) were also detected with the biotransformation

localized to the spiro oxetanylazetidinyl moiety in AZD1979. While M1 was a relatively minor

metabolite formed in HLM, it was the metabolite detected in the absence of NAD(P)H and

formed in comparable amounts as in the presence of NAD(P)H. M1 was not observed in negative

control incubations in the potassium phosphate buffer without HLM.

Mass spectra (Figure 1) of M1 exhibited MH$^+$ at *m/z* 481.2097 (molecular composition

$C_{25}H_{28}N_4O_6$, error 1 mDa) corresponding to the parent AZD1979 (molecular composition

$C_{25}H_{26}N_4O_5$) with the addition of a molecule of water. The MS/MS spectrum of M1 was

compared to the corresponding spectrum of AZD1979 (Figure 1). The major fragment ions of

both molecules were identical and were derived from the neutral loss of the spiro

oxetanylazetidinyl moiety of AZD1979, indicating that this moiety was the site of

biotransformation (net addition of H_2O to AZD1979). The most likely product would be either

diol **1** (net ring-opening addition of water to the oxetanyl group) or amino alcohol **2** (net ring-

opening addition of water to the azetidinyl group) (Figure 2). Because no fragment ion of M1

retained the spiro moiety, the MS data did not provide enough information to distinguish

between regioisomers **1** and **2**. The molecule AZ13478123 representing the structure shown as

regioisomer **1** was synthesized as described in Materials and Methods by acidic hydrolysis of

AZD1979 using sulphuric acid and was characterized by NMR (Supplemental Figure S1-S3 and

11

DMD # 71142

Tabel S1). Having this synthesized reference in hand two chemical correlations were performed

to confirm M1 is AZ13478123. First, the high resolution mass spectra obtained from synthesized

AZ13478123 and M1 were identical. Second, synthesized AZ13478123 co-eluted with M1 using

two significantly different LC chromatographic conditions (Supplemental Figure S4). Therefore,

we concluded that the chemical structure of M1 is the diol AZ13478123 formed by the net

hydration of the oxetanyl group of AZD1979.

Formation of metabolite M1 in human liver S9 fraction, microsomes and cytosol. With the

structure of M1 established, further characterization of the formation of this metabolite was

pursued. The ability of human liver S9 fraction, microsomes and cytosol to catalyze the net

hydration of the oxetanyl group of AZD1979 to a diol was examined. The formation of M1 was

observed in all liver subcellular fractions with HLM showing the highest activity (Figure 3)

indicating that the enzyme activity was mainly present in microsomes. Furthermore, the net

hydration of AZD1979 forming metabolite M1 was shown to be NAD(P)H-independent,

narrowing down the possible enzyme(s) involved in this reaction to those that do not require

NAD(P)H as a cofactor for catalytic activity and most likely involving a hydration rather than a

redox pathway. We therefore probed this question with the aid of labelled $H_2^{18}O$ and postulated

the involvement of microsomal epoxide hydrolase (mEH) on this metabolic pathway.

Incorporation of ^{18}O into metabolite M1 in $H_2^{18}O$ enriched HLM and S9 incubations. To

further assess the mechanism of the formation of M1, the incorporation of ^{18}O from $H_2^{18}O$

(77.6% ^{18}O) into M1 was studied following the incubation of AZD1979 in HLM and S9 fraction.

Analysis of the incubation mixtures produced high resolution mass spectra of M1 with isotopic

patterns characteristic of ^{18}O incorporation (Figure 4). MH$^+$ values of *m/z* 481.2108

($C_{25}H_{29}N_4^{16}O_6$, error 3 mDa), and *m/z* 483.2170 ($C_{25}H_{29}N_4^{16}O_5^{18}O$, error 4 mDa) were observed.

The abundance of the isotope peak representing ^{18}O incorporation was calculated using the

extracted MS peak at m/z 483.2170 subtracted by the +2 Da naturally occurring isotopic species

of $[^{16}O/^{13}C_2]M1$ (estimated as 4% of $[^{16}O]M1$, Figure 4), which could not be separated from

$[^{18}O]M1$ in the mass spectra. The ^{18}O incorporation rate was calculated using Eq 1.

$$\% \ ^{18}O \ Incorporation = \frac{[^{18}O]M1 - [^{16}O]M1 \times 4\%}{[^{16}O]M1 + ([^{18}O]M1 - [^{16}O]M1 \times 4\%)} \times 100\% \ \ (Eq.\ 1)$$

The accumulated ^{18}O-incorporation was time dependent with the highest values being 57% in S9

fraction and 29% in HLM following 2 hours incubation. Negative controls, where the

synthesized diol (AZ13478123), was incubated in $H_2{}^{18}O$ (77.6% ^{18}O) buffer without HLM or S9,

showed no net increase of ^{18}O content after a 2-hour incubation period.

pH-dependence of M1 formation following incubation of AZD1979 in HLM and S9

fraction. The maximum activity for the hydration reaction in HLM and S9 was established as

occurring between pH 8.5 and 9 (Figure 5). No M1 was detected in negative control incubations

under the same conditions without HLM or S9 fraction.

Kinetic analysis of M1 formation in HLM. Kinetic analyses of M1 formation were performed

in incubations of AZD1979 in HLM (Figure 6). The enzyme kinetic parameters, K_m and V_{max} for

M1 formation were calculated by fitting the data to the Michaelis-Menten equation. The

estimated K_m and V_{max} values were 542 µM and 118 pmol/min/mg, respectively. Thus, the

intrinsic clearance Cl_{int} (V_{max}/K_m) *via* this hydration pathway was 0.22 µL/min/mg in HLM.

Inhibition of M1 formation by chemical inhibitors of EH. Progabide and *t*-AUCB, inhibitors

of mEH and sEH, respectively (Kroetz et al., 1993; Liu et al., 2009), were examined for their

effects on M1 formation. The rate of the M1 formation was markedly decreased by progabide

13

following incubations of AZD1979 in HLM, S9 and cytosol (Figure 7). However, no inhibition

was observed by t-AUCB. The IC$_{50}$ value of progabide on M1 formation in HLM was

determined as 25.3 µM (Figure 8).

Discussion

Epoxide hydrolases (EH) are enzymes that catalyze the hydrolysis of epoxides and arene oxides to their corresponding diols. EHs are ubiquitous and the hydration of epoxide substrates is energetically favored, with water as the only co-substrate (Lacourciere and Armstrong, 1993; Hammock et al., 1994; Muller et al., 1997; Laughlin et al., 1998). In mammals, there are several EHs including soluble (sEH), microsomal (mEH) and cholesterol epoxide hydrolase (chEH), hepoxilin hydrolase and leukotriene A4 epoxide hydrolase (Kodani and Hammock, 2015). Among these EHs, sEH and mEH have been extensively characterized because of their potential clinical value and the involvement of mEH in the metabolism of xenobiotics (detoxification of cytotoxic, mutagenic and carcinogenic intermediates) (Morisseau and Hammock, 2005; El-Sherbeni and El-Kadi, 2014; Kodani and Hammock, 2015; Václavíková et al., 2015). The mEH is the key hepatic enzyme that catalyzes the hydration of numerous xenobiotics such as the epoxides of 1,3-butadiene, styrene, naphthalene, benzo(a)pyrene, phenantoin, and carbamazepine (El-Sherbeni and El-Kadi, 2014; Rosa et al., 2016). The sEH, on the other hand, appears to have a rather restricted substrate selectivity being involved in the metabolism of endogenous epoxides and has not been shown to hydrate any toxic or mutagenic xenobiotics (Morisseau and Hammock, 2013). Although phosphatase activity has recently been reported for sEH and mEH has been shown to have esterase activity in the metabolism of endogenous substrates (De Vivo et al., 2007; Nithipatikom et al., 2014), to the best of our knowledge xenobiotic substrates of mEH are limited to three-membered cyclic ethers, i.e. epoxides. In the present study, we show for the first time the mEH catalyzed hydration of an oxetanyl ring which is part of the spiro oxetanylazetidinyl moiety of AZD1979. The reaction which generated the corresponding diol product M1 establishes a new type of xenobiotic substrate for mEH.

Several recent publications have described the remarkable ability of oxetanyl moieties to modify

and improve the physicochemical and pharmacokinetic profiles of drug candidates, such as

solubility, basicity, lipophilicity, and metabolic stability (Wuitschik et al., 2008; Burkhard et al.,

2010; Wuitschik et al., 2010; Carreira and Fessard, 2014; Zheng et al., 2014). AZD1979 is a

MCHr1 antagonist containing a spiro oxetanylazetidinyl moiety as a building block. Contrary to

the reported P450-mediated oxidative ring scission of oxetanes (Stepan et al., 2011; Rioux et al.,

2016), our studies have shown that the net addition of water to AZD1979 to form M1 is a non-

P450 enzyme catalyzed reaction. Although the final diol products from these oxetanes are

analogous, the mechanisms which lead to their formation are clearly different. The diol

metabolite M1 was also detected in human hepatocyte incubations and the plasma from

preclinical species (unpublished data). Therefore, it was important to understand this unusual

metabolic reaction and to characterize the enzyme(s) involved. Our studies have shown the

NAD(P)H-independent formation of M1 in HLM, cytosol and S9 fraction, with the highest

catalytic activity being detected in HLM. These results establish that the net hydration of the

oxetanyl moiety in AZD1979 was not catalyzed by an NAD(P)H-dependent oxidoreductase,

such as P450 and FMO, a process that would proceed initially *via* oxidation followed by

reduction of the resulting 2-electron oxidation product. The incorporation of ^{18}O into M1 was

consistent with the incorporated oxygen originating from water (not dioxygen). Therefore, this

biotransformation is mechanistically classified as proceeding *via* a hydrolytic rather than a redox

process. In addition, the chemical structure of M1 and the hepatic enzyme activities that catalyse

this hydration reaction led us to postulate that the formation of M1 was mediated by the mEH.

We suggest that the low formation of M1 in the cytosolic preparation results from residual mEH
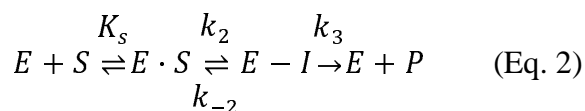
activity in cytosol (Thomas et al., 1990).

To further clarify the potential role of mEH as the catalyst in the hydration of the oxetanyl ring of AZD1979, the effect of chemical inhibitors on M1 formation was investigated by using progabide, a potent inhibitor of mEH, and *t*-AUCB, a potent inhibitor of sEH. Over 80% inhibition of M1 formation by progabide was observed with an IC_{50} value of 25.3 µM. This was comparable with the reported IC_{50} value (19.7 µM) for progabide inhibition on the hydration of styrene oxide, an mEH marker reaction in HLM (Nicolas et al., 1999). By contrast, *t*-AUCB did not significantly inhibit the formation of M1 in any incubation, indicating the minimal contribution by sEH.

The mEHs belong to the α/β-fold hydrolase family of enzymes, which are characterized as a nucleophile-histidine-acid catalytic triad and function *via* a two-step mechanism formin*g* a covalent intermediate, i.e. a hydroxylalkyl-enzyme intermediate (Armstrong and Cassidy, 2000; Morisseau and Hammock, 2005). Based on the established mechanism of EH catalyzed hydration (Lacourciere and Armstrong, 1993; Huey-Fen Tzeng, 1996; Laughlin et al., 1998; Armstrong, 1999), a modified pathway for the mEH-catalyzed hydration of the oxetanyl moiety in AZD1979 is proposed (Figure 9). As illustrated in Figure 9, the oxygen that is incorporated into the product diol is derived from one of two sources, the carboxylate from mEH in the single turnover reaction and from H_2O in the proceeding reactions. Lacourcier and Armstrong reported that the mEH-catalyzed hydration of phenanthrene 9,10-oxide in $H_2^{18}O$ under single-turnover conditions in the presence of excess enzyme gave very little incorporation of ^{18}O in the product trans-9,10-dihydro-9,10-dihydroxylphenanthrene(Lacourciere and Armstrong, 1993) (Lacourciere and Armstrong, 1993). In contrast, under multiple-turnover reaction conditions (substrate in excess) the expected appearance of ^{18}O in the product was observed (Lacourciere and Armstrong, 1993). This mechanism explains the sub-maximal incorporation of ^{18}O into M1

DMD # 71142

(57% in S9 fraction and 29% in HLM) compared to the abundance of $H_2^{18}O$ (77.6% ^{18}O) in the incubation medium. The lower incorporation rate in HLM, as compared to that in S9 fraction, can be explained by the higher mEH concentration in HLM, where the single-turnover condition dominated over the multiple-turnover reaction. This led to a higher incorporation of ^{16}O from the carboxylate of mEH, rather than of ^{18}O from the water.

The kinetic constants for M1 formation from AZD1979 were estimated from fitting the data to the Michaelis-Menten equation revealing a K_m of 542 µM in HLM. In contrast to P450-catalyzed reactions, the mechanism of EH-catalyzed hydrolysis involving the formation of a covalent intermediate has been described by a simplified kinetic mechanism shown in Eq. 2. Rapid equilibrium binding (K_s) of the substrate to form a Michaelis complex is followed by reversible formation of the ester intermediate (k_2/k_{-2}) and essentially irreversible hydrolysis (k_3) of the intermediate (E-I), as the rate-limiting step (Hammock et al., 1994; Huey-Fen Tzeng, 1996); (Yamada et al., 2000).

$$E + S \underset{}{\overset{K_s}{\rightleftharpoons}} E \cdot S \underset{k_{-2}}{\overset{k_2}{\rightleftharpoons}} E - I \overset{k_3}{\rightarrow} E + P \qquad \text{(Eq. 2)}$$

Therefore, the apparent K_m is not a measure of the affinity of the substrate to the enzyme, but rather a reflection of the substrate concentration for which the formation velocity is half-maximal. Oesch et al. demonstrated that the efficiency of the EH-mediated hydrolysis of epoxides was underestimated based on the observed overall rate of dihydrodiol formation (Oesch et al., 2000; Oesch et al., 2004). In fact, epoxides are rapidly trapped by forming covalent ester intermediates (E-I) without any significant formation of dihydrodiol. Considering the mechanism of the mEH-catalyzed hydration of the oxetanyl moiety of AZD1979, the low turnover number

18

of M1 formation (V_{max} of 118 pmol/min/mg in HLM) does not necessarily reflect the efficiency of catalytic activity of the mEH.

The nucleophilic carboxylate of aspartic acid (Asp[226]) in the mEH active site is thought to be the target binding site for the formation of the hydroxylalkyl-enzyme intermediate, which is then hydrolysed by an activated water molecule to release the diol product and regenerate the enzyme (Morisseau and Hammock, 2005). The water molecule activation requires a non-protonated histidine (His[431]) residue, also located in the active site of mEH, which acts as a general base in the hydrolysis of the ester (Pinot et al., 1995; Laughlin et al., 1998; Armstrong, 1999; Morisseau and Hammock, 2005). The optimal pH of 8.5 to 9.0 for M1 formation in our study is consistent with the reported optimal pH of recombinant human mEH-catalyzed reactions (pH 8 to 9) (Dansette et al., 1978), and is in agreement with the characteristics of mEH to satisfy both the Asp and His involvement in intermediate formation and ester hydrolysis.

Unlike many hydrolytic or group transfer reactions that occur *via* covalent intermediates, during the EH mediated two-step reaction the bond made during the formation of the hydroxylalkyl-enzyme intermediate is not the same bond that undergoes hydrolysis to release the final diol product (Figure 9). The ease by which these bonds can be formed and hydrolytically cleaved is reflected in the velocities of substrate depletion and of diol product formation. The chemical properties of the substrate play an important role in the mEH-mediated reaction. Following the current finding that an oxetane ring is a novel mEH substrate, it is of particular interest to investigate the chemical space of oxetanyl-containing compounds and their substituted analogues and to understand the structural features determining the specificity for oxetane ring opening mediated by P450s versus mEH. In addition, interindividual and interspecies variation in hepatic mEH activity have also been reported (Kitteringham et al., 1996). Therefore, particular care

should be taken with those oxetanyl-containing chemical entities that are substrates of mEH, regarding risk-benefit assessment in drug discovery and development. Investigations on the structure-activity relationships for oxetanyl derivatives by mEH-catalyzed hydration are ongoing, and findings from these studies will be disclosed in forthcoming publications.

In conclusion, our study reports a novel mEH-catalyzed ring-opening hydration of an oxetane that is part of a spiro oxetanylazetidinyl moiety in AZD1979 forming the corresponding diol metabolite. This reaction describes a new class of substrates for mEH.

DMD # 71142

Acknowledgments

Authorship Contributions

Participated in research design: Li, Hayes, Castagnoli Jr., and Weidolf

Conducted experiment: Li, Grönberg and Berggren

Performed data analysis: Li, Grönberg and Berggren

Wrote or contributed to the writing of the manuscript: Li, Hayes, Grönberg, Berggren, Castagnoli Jr., and Weidolf

DMD # 71142

References

Armstrong RN (1999) Kinetic and chemical mechanism of epoxide hydrolase. *Drug Metab Rev* **31:**71-86.

Armstrong RN and Cassidy CS (2000) New structural and chemical insight into the catalytic mechanism of epoxide hydrolases. *Drug Metab Rev* **32:**327-338.

Burkhard JA, Wuitschik G, Plancher JM, Rogers-Evans M, and Carreira EM (2013) Synthesis and stability of oxetane analogs of thalidomide and lenalidomide. *Org Lett* **15:**4312-4315.

Burkhard JA, Wuitschik G, Rogers-Evans M, Muller K, and Carreira EM (2010) Oxetanes as versatile elements in drug discovery and synthesis. *Angew Chem Int Ed* **49:**9052 – 9067.

Carreira EM and Fessard TC (2014) Four-membered ring-containing spirocycles: synthetic strategies and opportunities. *Chem Rev* **114:**8257-8322.

Dansette PM, Makedonska VB, and Jerina DM (1978) Mechanism of catalysis for the hydration of substituted styrene oxides by hepatic epoxide hydrase. *Arch Biochem Biophys* **187:**290-298.

De Vivo M, Ensing B, Dal Peraro M, Gomez GA, Christianson DW, and Klein ML (2007) Proton shuttles and phosphatase activity in soluble epoxide hydrolase. *J Am Chem Soc* **129:**387-394.

El-Sherbeni AA and El-Kadi AO (2014) The role of epoxide hydrolases in health and disease. *Arch Toxicol* **88:**2013-2032.

Fretland AJ and Omiecinski CJ (2000) Epoxide hydrolases: biochemistry and molecular biology. *Chem Biol Interact* **129:**41-59.

Hammock BD, Pinot F, Beetham JK, Grant DF, Arand ME, and Oesch F (1994) Isolation of a putative hydroxyacyl enzyme intermediate of an epoxide hydrolase. *Biochem Biophys Res Commun* **198:**850-856.

Huey-Fen Tzeng LTL, Sue Lin, and Richard N. Armstrong (1996) The catalytic mechanism of microsomal epoxide hydrolase involves reversible formation and rate-limiting hydrolysis of the alkyl-enzyme intermediate. *J Am Chem Soc* **118:**9436-9437.

Hutzler JM, Obach RS, Dalvie D, and Zientek MA (2013) Strategies for a comprehensive understanding of metabolism by aldehyde oxidase. *Expert Opin Drug Metab Toxicol* **9:**153-168.

Hwang SH, Tsai H-J, Liu J-Y, Morisseau C, and Hammock BD (2007) Orally bioavailable potent soluble epoxide hydrolase inhibitors. *J Med Chem* **50:**3825-3840.

Inoue H, Castagnoli K, Van Der Schyf C, Mabic S, Igarashi K, and Castagnoli N, Jr. (1999) Species-dependent differences in monoamine oxidase A and B-catalyzed oxidation of various C4 substituted 1-methyl-4-phenyl-1,2,3, 6-tetrahydropyridinyl derivatives. *J Pharmacol Exp Ther* **291:**856-864.

Johansson A, Lofberg C, Antonsson M, von Unge S, Hayes MA, Judkins R, Ploj K, Benthem L, Linden D, Brodin P, Wennerberg M, Fredenwall M, Li L, Persson J, Bergman R, Pettersen A, Gennemark P, and Hogner A (2016) Discovery of (3-(4-(2-oxa-6-azaspiro[3.3]heptan-6-ylmethyl)phenoxy)azetidin-1-yl)(5-(4-methoxy phenyl)-1,3,4-oxadiazol-2-yl)methanone (AZD1979), a melanin concentrating hormone receptor 1 (MCHr1) antagonist with favorable physicochemical properties. *J Med Chem* **59:**2497-2511.

DMD # 71142

Kitteringham NR, Davis C, Howard N, Pirmohamed M, and Park BK (1996) Interindividual and interspecies variation in hepatic microsomal epoxide hydrolase activity: studies with cis-stilbene oxide, carbamazepine 10, 11-epoxide and naphthalene. *J Pharmacol Exp Ther* **278:**1018-1027.

Kodani SD and Hammock BD (2015) The 2014 Bernard B. Brodie award lecture-epoxide hydrolases: drug metabolism to therapeutics for chronic pain. *Drug Metab Dispos* **43:**788-802.

Kroetz DL, Loiseau P, Guyot M, and Levy RH (1993) In vivo and in vitro correlation of microsomal epoxide hydrolase inhibition by progabide. *Clin Pharmacol Ther* **54:**485-497.

Lacourciere GM and Armstrong RN (1993) The catalytic mechanism of microsomal epoxide hydrolase involves an ester intermediate. *J Am Chem Soc* **115:**10466-10467.

Laughlin LT, Tzeng HF, Lin S, and Armstrong RN (1998) Mechanism of microsomal epoxide hydrolase. Semifunctional site-specific mutants affecting the alkylation half-reaction. *Biochemistry* **37:**2897-2904.

Liu JY, Park SH, Morisseau C, Hwang SH, Hammock BD, and Weiss RH (2009) Sorafenib has soluble epoxide hydrolase inhibitory activity, which contributes to its effect profile in vivo. *Mol Cancer Ther* **8:**2193-2203.

Morisseau C and Hammock BD (2005) Epoxide hydrolases: mechanisms, inhibitor designs, and biological roles. *Annu Rev Pharmacol Toxicol* **45:**311-333.

Morisseau C and Hammock BD (2013) Impact of soluble epoxide hydrolase and epoxyeicosanoids on human health. *Annu Rev Pharmacol Toxicol* **53:**37-58.

Muller F, Arand M, Frank H, Seidel A, Hinz W, Winkler L, Hanel K, Blee E, Beetham JK, Hammock BD, and Oesch F (1997) Visualization of a covalent intermediate between microsomal epoxide hydrolase, but not cholesterol epoxide hydrolase, and their substrates. *Eur J Biochem* **245:**490-496.

Nicolas JM, Collart P, Gerin B, Mather G, Trager W, Levy R, and Roba J (1999) In vitro evaluation of potential drug interactions with levetiracetam, a new antiepileptic agent. *Drug Metab Dispos* **27:**250-254.

Nithipatikom K, Endsley MP, Pfeiffer AW, Falck JR, and Campbell WB (2014) A novel activity of microsomal epoxide hydrolase: metabolism of the endocannabinoid 2-arachidonoylglycerol. *J Lipid Res* **55:**2093-2102.

Oesch F, Hengstler JG, and Arand M (2004) Detoxication strategy of epoxide hydrolase-the basis for a novel threshold for definable genotoxic carcinogens. *Nonlinearity Biol Toxicol Med* **2:**21-26.

Oesch F, Herrero ME, Hengstler JG, Lohmann M, and Arand M (2000) Metabolic detoxification: implications for thresholds. *Toxicol Pathol* **28:**382-387.

Pinot F, Grant DF, Beetham JK, Parker AG, Borhan B, Landt S, Jones AD, and Hammock BD (1995) Molecular and biochemical evidence for the involvement of the Asp-333-His-523 pair in the catalytic mechanism of soluble epoxide hydrolase. *J Biol Chem* **270:**7968-7974.

Radominska-Pandya A, Czernik PJ, Little JM, Battaglia E, and Mackenzie PI (1999) Structural and functional studies of UDP-glucuronosyltransferases. *Drug Metab Rev* **31:**817-899.

Rendic S and Guengerich FP (2015) Survey of human oxidoreductases and cytochrome P450 enzymes involved in the metabolism of xenobiotic and natural chemicals. *Chem Res Toxicol* **28:**38-42.

Rioux N, Duncan KW, Lantz RJ, Miao X, Chan-Penebre E, Moyer MP, Munchhof MJ, Copeland RA, Chesworth R, and Waters NJ (2016) Species differences in metabolism of EPZ015666, an oxetane-containing protein arginine methyltransferase-5 (PRMT5) inhibitor. *Xenobiotica* **46:**268–277.

Rosa M, Bonnaillie P, and Chanteux H (2016) Prediction of drug-drug interactions with carbamazepine-10,11-epoxide using a new in vitro assay for epoxide hydrolase inhibition. *Xenobiotica* doi. 10.3109/00498254.2016.1151088.

Schwaninger AE, Meyer MR, and Maurer HH (2011) Investigation on the enantioselectivity of the sulfation of the methylenedioxymethamphetamine metabolites 3,4-dihydroxymethamphetamine and 4-hydroxy-3-methoxymethamphetamine using the substrate-depletion approach. *Drug Metab Dispos* **39:**1998-2002.

Scott JS, Birch AM, Brocklehurst KJ, Brown HS, Goldberg K, Groombridge SD, Hudson JA, Leach AG, MacFaul PA, McKerrecher D, Poultney R, Schofield P, and Svensson PH (2013) Optimisation of aqueous solubility in a series of G protein coupled receptor 119 (GPR119) agonists. *Med Chem Comm* **4:**95-100.

Stepan AF, Karki K, McDonald WS, Dorff PH, Dutra JK, Dirico KJ, Won A, Subramanyam C, Efremov IV, O'Donnell CJ, Nolan CE, Becker SL, Pustilnik LR, Sneed B, Sun H, Lu Y, Robshaw AE, Riddell D, O'Sullivan TJ, Sibley E, Capetta S, Atchison K, Hallgren AJ, Miller E, Wood A, and Obach RS (2011) Metabolism-directed design of oxetane-

containing arylsulfonamide derivatives as gamma-secretase inhibitors. *J Med Chem* **54:**7772-7783.

Thomas H, Timms CW, and Oesch F (1990) Epoxide hydrolases: Molecular properties, induction, polymorphisms and function., in *Frontiers in Biotransformation* (Ruckpaul K and Rein H eds), pp 278–337, Akademie-Verlag, Berlin.

Usmani KA, Chen WG, and Sadeque AJ (2012) Identification of human cytochrome P450 and flavin-containing monooxygenase enzymes involved in the metabolism of lorcaserin, a novel selective human 5-hydroxytryptamine 2C agonist. *Drug Metab Dispos* **40:**761-771.

Václavíková R, Hughes DJ, and Souček P (2015) Microsomal epoxide hydrolase 1 (EPHX1): Gene, structure, function, and role in human disease. *Gene* **571:**1-8.

Wu B and Dong D (2012) Human cytosolic glutathione transferases: structure, function, and drug discovery. *Trends Pharmacol Sci* **33:**656-668.

Wuitschik G, Carreira EM, Wagner B, Fischer H, Parrilla I, Schuler F, Rogers-Evans M, and Muller K (2010) Oxetanes in drug discovery: structural and synthetic insights. *J Med Chem* **53:**3227-3246.

Wuitschik G, Rogers-Evans M, Buckl A, Bernasconi M, Marki M, Godel T, Fischer H, Wagner B, Parrilla I, Schuler F, Schneider J, Alker A, Schweizer WB, Muller K, and Carreira EM (2008) Spirocyclic oxetanes: synthesis and properties. *Angew Chem Int Ed Engl* **47:**4512-4515.

Yamada T, Morisseau C, Maxwell JE, Argiriadi MA, Christianson DW, and Hammock BD (2000) Biochemical evidence for the involvement of tyrosine in epoxide activation during the catalytic cycle of epoxide hydrolase. *J Biol Chem* **275:**23082-23088.

DMD # 71142

Zheng Y, Tice CM, and Singh SB (2014) The use of spirocyclic scaffolds in drug discovery.

Bioorg Med Chem Lett **24:**3673-3682.

Figure Legends

Figure 1. MS/MS product ion spectra acquired by collision induced dissociation of the respective MH$^+$ ions of AZD1979 (top) and M1 (bottom). Insets are the tentative fragmentation pattern and the full scan MS spectra.

Figure 2. Proposed potential structure (**1** or **2**) of hydrated metabolite M1 of AZD1979.

Figure 3. NAD(P)H-dependence of the formation of M1. AZD1979 (10 µM) was incubated with various human liver subcellular fractions (1 mg/mL protein), with and without the presence of 1 mM mixture of NADPH-NADH over 60 minutes. Results are averages of duplicate. Mean of M1 formation in HLM incubations ±NAD(P)H was set as 100% abundance.

Figure 4. HRMS spectra of M1 in human liver S9 fraction incubated with AZD1979 (10 µM) for 120 min, with (A) and without (B) H$_2$^{18}O (77.6% ^{18}O) enrichment. Inset shows the time course of the accumulated incorporation of ^{18}O in M1 in human liver S9 or HLM.

Figure 5. Effect of pH on M1 formation in the incubation of AZD1979 (50 µM) with HLM or S9 fraction over 60 minutes. Results are averages of duplicate measurements.

Figure 6. Kinetics of the formation of M1 in HLM. A range of AZD1979 concentrations was incubated in HLM at 37°C for 30 minutes. The velocity (pmol/min/mg protein) versus concentration curve was fitted to a single-site Michaelis-Menten equation.

Figure 7. Effect of progabide on M1 formation following incubation of AZD1979 (10 µM) in human liver S9 fraction, cytosol and microsomes. Results are averages of duplicate measurements.

Figure 8. Inhibition effect of progabide on M1 formation after 30 min incubation of AZD1979

(200 µM) in human liver microsomes. Activity is expressed as a percentage of control activity

measured in the absence of inhibitor. IC50 values were determined by non-linear regression.

Figure 9. Proposed pathways for the mEH-catalyzed hydration of the oxetanyl moiety of

AZD1979 and related incorporation of oxygen from water into mEH and product diol. The

single-turnover and the subsequent reactions are shown to illustrate the origin of the additional

oxygen incorporated in the diol product. The oxygen atom originating from mEH is shown in

blue and that from water in the medium is in red. In the hydroxylalkyl-enzyme intermediate, the

new covalent bond formed is in yellow and the bond cleaved to release the final diol product is in

green. H^+ in the cycle represents proton transfer steps that are not shown.
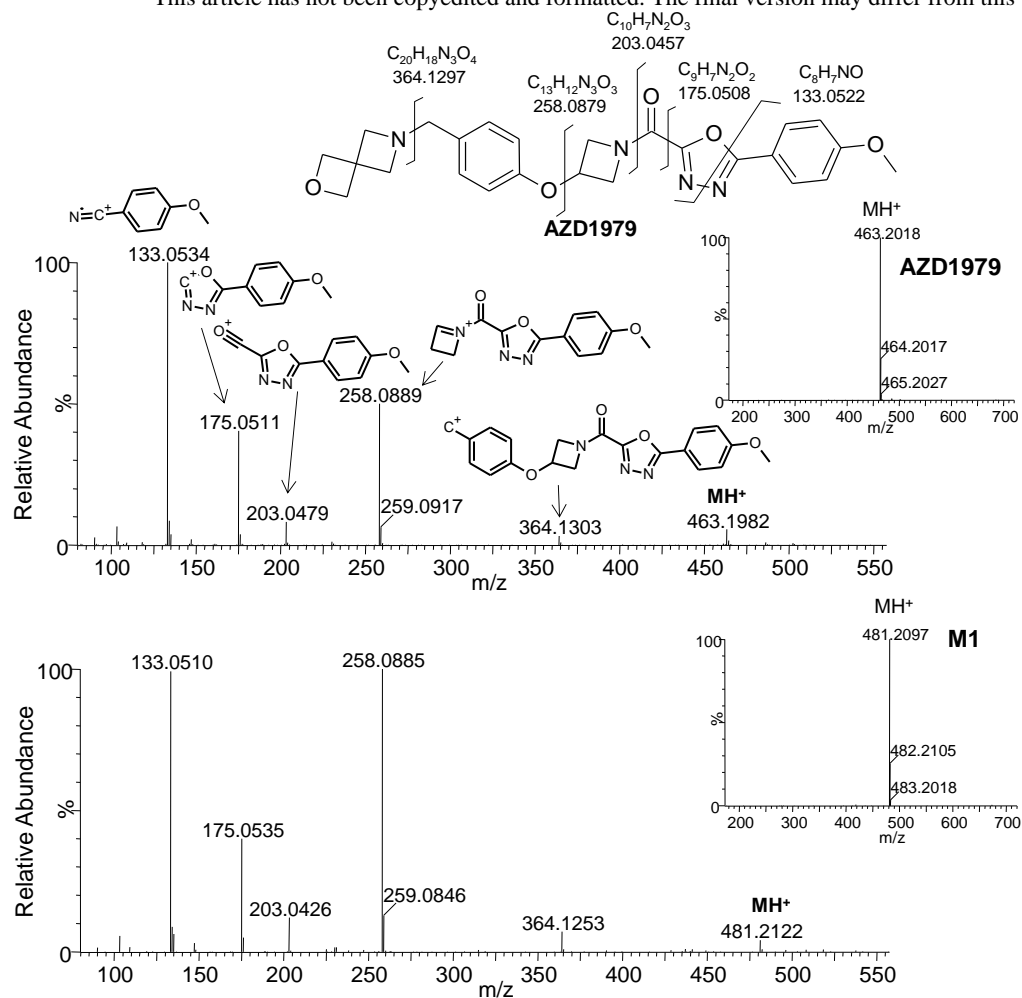
Figure 1.
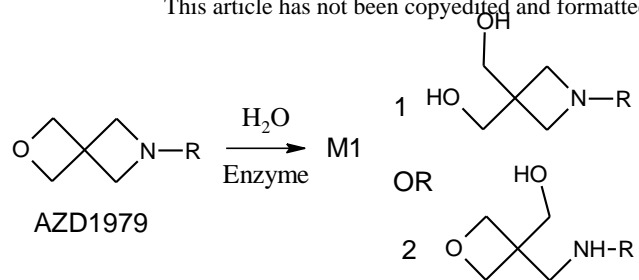
Figure 2.
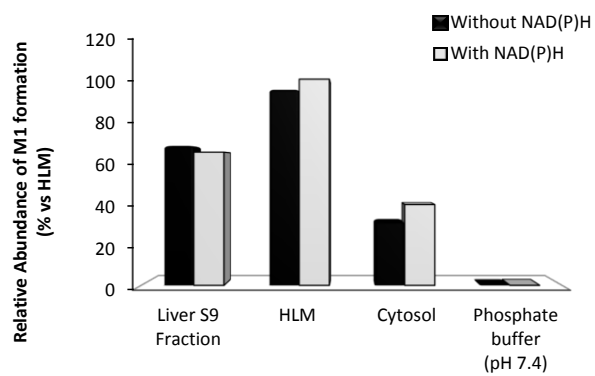
Figure 3.
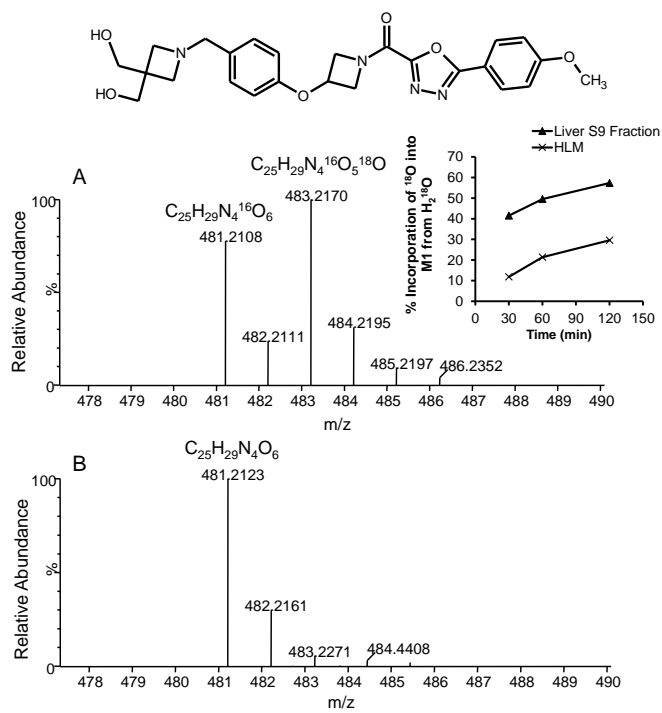
Figure 4.
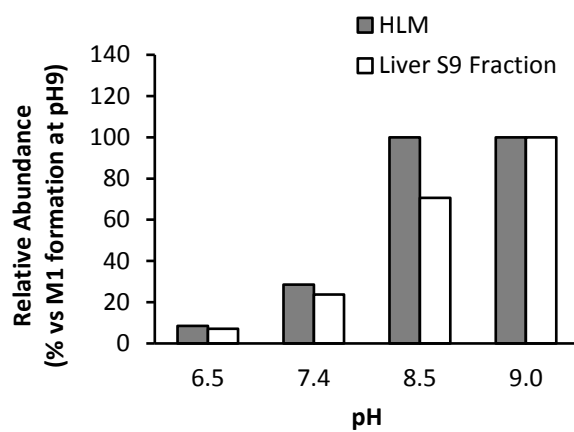
Figure 5.
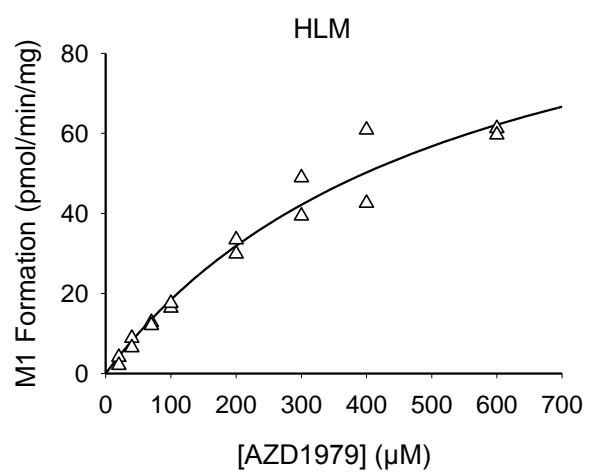
Figure 6.
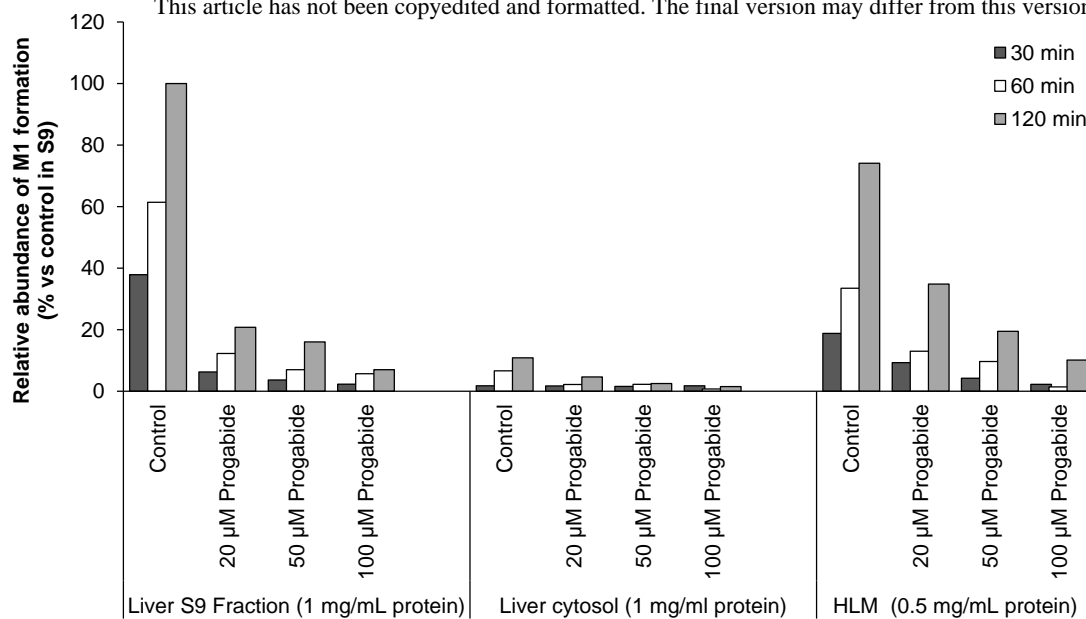
Figure 7.

Figure 8.

Figure 9.